Two-dimensional optical three-pulse photon echo spectroscopy. I. Nonperturbative approach to the calculation of spectra

Cite as: J. Chem. Phys. **124**, 234504 (2006); https://doi.org/10.1063/1.2200704
Submitted: 02 May 2005 . Accepted: 06 April 2006 . Published Online: 16 June 2006

Tomáš Mančal, Andrei V. Pisliakov, and Graham R. Fleming

Two-dimensional optical three-pulse photon echo spectroscopy. I. Nonperturbative approach to the calculation of spectra

Tomáš Mančal, Andrei V. Pisliakov, and Graham R. Fleming[a)]
Department of Chemistry, University of California, Berkeley, California 94720
and Physical Biosciences Division, Lawrence Berkeley National Laboratory, Berkeley, California 94720

(Received 2 May 2005; accepted 6 April 2006; published online 16 June 2006)

The nonperturbative approach to the calculation of nonlinear optical spectra of Seidner *et al.* [J. Chem. Phys. **103**, 3998 (1995)] is extended to describe four-wave mixing experiments. The system-field interaction is treated nonperturbatively in the semiclassical dipole approximation, enabling a calculation of third order nonlinear spectroscopic signals directly from molecular dynamics and an efficient modeling of multilevel systems exhibiting relaxation and transfer phenomena. The method, coupled with the treatment of dynamics within the Bloch model, is illustrated by calculations of the two-dimensional three-pulse photon echo spectra of a simple model system—a two-electronic-level molecule. The nonperturbative calculations reproduce well-known results obtained by perturbative methods. Technical limitations of the nonperturbative approach in dealing with a dynamic inhomogeneity are discussed, and possible solutions are suggested. An application of the approach to an excitonically coupled dimer system with emphasis on the manifestation of complex exciton dynamics in two-dimensional optical spectra is presented in paper II Pisliakov *et al.* [J. Chem. Phys. **124**, 234505 (2006), following paper]. © *2006 American Institute of Physics*. [DOI: 10.1063/1.2200704]

I. INTRODUCTION

Nonlinear spectroscopy is an increasingly important tool for studying the dynamics and structure of molecular systems on the femtosecond time scale. An impressive progress in infrared (IR) spectroscopy with the establishment of new multidimensional methods to probe vibrational dynamics and couplings[1–10] has been followed by descriptions of a visible-domain heterodyne detection of nonlinear signals and two-dimensional photon echo measurements,[11–22] optical phase cycling on atoms,[23] and very recently two-dimensional photon echo spectra measurements of the biologically relevant Fenna-Matthews-Olson (FMO) complex.[24,25]

The conventional approach[26–29] to the theory of nonlinear spectroscopy, which utilizes a perturbative expansion of the system dynamics in orders of the external electric field, is convenient and efficient, provided that the nonlinear response functions can be evaluated analytically. This is possible even for multilevel systems[26,28,29] in interaction with a bath of harmonic oscillators, given that no population transfer between the levels is induced by this bath. When the number of states increases and the dynamics of the molecular system requires a more complex description, the perturbative formalism can be used in the form of a doorway-window picture[26] that utilizes the system propagation for the calculation of nonlinear response functions. In this paper we provide an extension of an alternative method[30] that avoids an evaluation of response functions and calculates the nonlinear signal directly from the system dynamics.

Several decades of research in the field of open quantum systems[31,32] provide a number of methods and approaches that enable the calculation of the time evolution of complex systems. These methods range from rigorous quantum-mechanical methods (for review, see Ref. 33) to a semiclassical initial value representation method (see, e.g., Refs. 34 and 35) or stochastic wave function propagation.[34–39] Typically, the dissipative effects in multistate systems are described by the numerical propagation of the reduced density matrix via the Redfield equation.[40,41] When using these methods, it is logical and often more straightforward to implement a direct numerical treatment of the system-field interaction in order to avoid the evaluation of the multiple system response functions. The main advantage of the nonperturbative (NP) approach, introduced in Ref. 30 and extended in this paper, is that it enables calculation of nonlinear optical signals directly from the system dynamics when using the above mentioned theoretical methods. The system-field interaction is treated (numerically) exactly by its explicit inclusion into the total Hamiltonian

$$H_{\mathrm{tot}}(t) = H_{\mathrm{mol}} - \boldsymbol{\mu} \cdot \mathbf{n}\mathcal{E}(t), \tag{1}$$

where $\boldsymbol{\mu}$ is the system transition dipole operator, $\mathcal{E}(t)$ is the external (laser) electric field, and $\mathbf{n}$ is a unity vector in the direction of the field polarization. The total optical polarization, which is the key quantity for the calculation of spectroscopic signals, is obtained as an expectation value of the dipole moment operator $\boldsymbol{\mu}$ [see Eq. (5)].

Depending on the geometry of the experiment, the contributions corresponding to different orders of the nonlinear response are usually distinguishable by the direction of the emitted field. In a computer simulation, only the overall polarization is produced, and no directional information is retained. The key to the NP method is the ability to extract the

a)Electronic mail: grfleming@lbl.gov

[53] A. A. Ferro, J. D. Hybl, and D. M. Jonas, J. Chem. Phys. **114**, 4649 (2001).
[54] F. Bloch, Phys. Rev. **70**, 460 (1946).
[55] R. Agarwal, A. H. Rizvi, B. S. Prall, J. D. Olsen, C. N. Hunter, and G. R. Fleming, J. Phys. Chem. A **106**, 7573 (2002).
[56] M. Yang, R. Agarwal, and G. R. Fleming, J. Photochem. Photobiol., A **142**, 107 (2001).
[57] M. Yang and G. R. Fleming, J. Chem. Phys. **113**, 2823 (2000).
[58] M. Yang, K. Ohta, and G. R. Fleming, J. Chem. Phys. **110**, 10243 (1999).
[59] W. H. Press, B. P. Flannery, S. A. Teukolsky, and W. T. Vetterling, *Numerical Recipes* (Cambridge University Press, Cambridge, 1986).
[60] M. Cho, N. F. Scherer, G. R. Fleming, and S. Mukamel, J. Chem. Phys. **96**, 5618 (1992).
[61] T. Joo, Y. Jia, J.-Y. Yu, J. Lang, and G. R. Fleming, J. Chem. Phys. **104**, 6089 (1996).
[62] A. Tokmakoff, J. Phys. Chem. A **104**, 4247 (2000).
[63] G. R. Fleming and M. Cho, Annu. Rev. Phys. Chem. **47**, 109 (1996).
[64] P. Geissler (private communication).

tories where the energy gap evolves in time. In fact, such methods exist and are usually termed stochastic wave function or Monte Carlo wave function methods (MCWM).[36–39] In the MCWM, an ensemble of wave functions is propagated, and the influence of the environment on the wave functions is simulated by allowing "quantum jumps" between the eigenstates of the system. For these methods, the implementation of the nonperturbative algorithm does not represent any additional calculations of system dynamics. Stochastic methods scale only linearly with the size of the system and provide a description of a system-bath interaction that is equivalent to the density matrix description for certain types of relaxation operators. Since all observables, including the polarization, are evaluated by averaging over the ensemble of wave functions (molecules), the problems that lead to the failure of the NP method to include a dynamic inhomogeneity are naturally avoided in the stochastic propagation. Therefore, we propose that the NP approach with a stochastic wave function method could represent an ideal method for calculating nonlinear optical signals. This topic will be addressed in more detail elsewhere.

VII. CONCLUSIONS

In this paper we have developed a nonperturbative approach to calculate nonlinear spectroscopic signals in three pulse experiments. We have established a method to extract the directional components of an arbitrary order optical polarization in four-wave mixing experiments on electronic systems with an arbitrary number of levels. The method has been implemented to obtain the direction-resolved components for third order signals.

We have illustrated the method by calculating the two-dimensional photon echo spectra of a model two-level system. The spectral features established previously within a perturbative theoretical framework have been reproduced by our nonperturbative calculations. We have demonstrated that by means of averaging over a fluctuating energy gap one may overcome difficulties of treating the dynamic inhomogeneity within the nonperturbative approach. We also suggested the nonperturbative approach be used with the stochastic wave function approach where it does not represent an additional computational overhead to the method.

ACKNOWLEDGMENTS

The authors thank Phillip Geissler for incisive comments on spectral diffusion and Elizabeth L. Read for helpful comments on the text. This work was supported by a grant from NSF.

[1] P. Hamm, M. Lim, and R. M. Hochstrasser, J. Phys. Chem. B **102**, 6123 (1998).
[2] P. Hamm, M. Lim, W. F. DeGrado, and R. M. Hochstrasser, J. Phys. Chem. A **103**, 10049 (1999).
[3] M. C. Asplund, M. T. Zanni, and R. M. Hochstrasser, Proc. Natl. Acad. Sci. U.S.A. **97**, 8219 (2000).
[4] N.-H. Ge, M. T. Zanni, and R. M. Hochstrasser, J. Phys. Chem. A **106**, 962 (2002).
[5] C. Fang, J. Wang, A. K. Charnley, W. Barber-Armstrong, A. B. Smith III, S. M. Decatur, and R. M. Hochstrasser, Chem. Phys. Lett. **382**, 586 (2003).
[6] M. Khalil and A. Tokmakoff, Chem. Phys. **266**, 213 (2001).
[7] N. Demirdoven, M. Khalil, and A. Tokmakoff, Phys. Rev. Lett. **89**, 237401 (2002).
[8] M. Khalil, N. Demirdoven, and A. Tokmakoff, J. Phys. Chem. A **107**, 5258 (2003).
[9] M. Khalil, N. Demirdoven, and A. Tokmakoff, Phys. Rev. Lett. **90**, 047401 (2003).
[10] M. Khalil, N. Demirdoven, and A. Tokmakoff, J. Chem. Phys. **121**, 362 (2004).
[11] L. Lepetit and M. Joffre, Opt. Lett. **21**, 564 (1996).
[12] J.-P. Likforman, M. Joffre, and V. Thierry-Mieg, Opt. Lett. **22**, 1104 (1997).
[13] N. Belabas and M. Joffre, Opt. Lett. **27**, 2043 (2002).
[14] S. M. G. Faeder, A. W. Albrecht, J. D. Hybl, B. L. Landin, B. Rajaram, and D. M. Jonas, J. Opt. Soc. Am. B **15**, 2338 (1998).
[15] J. D. Hybl, A. W. Albrecht, S. M. G. Faeder, and D. M. Jonas, Chem. Phys. Lett. **297**, 307 (1998).
[16] S. M. G. Faeder and D. M. Jonas, J. Phys. Chem. A **103**, 10489 (1999).
[17] J. D. Hybl, A. A. Ferro, and D. M. Jonas, J. Chem. Phys. **115**, 6606 (2001).
[18] J. D. Hybl, A. Yu, D. A. Farrow, and D. M. Jonas, J. Phys. Chem. A **106**, 7651 (2002).
[19] D. M. Jonas, Annu. Rev. Phys. Chem. **54**, 425 (2003).
[20] M. L. Cowan, J. P. Ogilvie, and R. J. D. Miller, Chem. Phys. Lett. **386**, 184 (2004).
[21] T. Brixner, I. V. Stiopkin, and G. R. Fleming, Opt. Lett. **29**, 884 (2004).
[22] T. Brixner, T. Mančal, I. V. Stiopkin, and G. R. Fleming, J. Chem. Phys. **121**, 4221 (2004).
[23] P. Tian, D. Keusters, Y. Suzaki, and W. S. Warren, Science **300**, 1553 (2003).
[24] T. Brixner, J. Stenger, H. M. Vaswani, M. Cho, R. E. Blankenship, and G. R. Fleming, Nature (London) **434**, 625 (2005).
[25] M. Cho, H. M. Vaswani, T. Brixner, J. Stenger, and G. R. Fleming, J. Phys. Chem. B **109**, 10542 (2005).
[26] S. Mukamel, *Principles of Nonlinear Optical Spectroscopy* (Oxford University Press, New York, 1995).
[27] W. Domcke and G. Stock, Adv. Chem. Phys. **100**, 1 (1997).
[28] J. Sung and R. J. Silbey, J. Chem. Phys. **115**, 9266 (2001).
[29] J. Sung and R. J. Silbey, J. Chem. Phys. **118**, 2443 (2003).
[30] L. Seidner, G. Stock, and W. Domcke, J. Chem. Phys. **103**, 3998 (1995).
[31] U. Weiss, *Quantum Dissipative Systems* (World Scientific, Singapore, 1993).
[32] V. May and O. Kühn, *Charge and Energy Transfer Dynamics in Molecular Dynamics* (Wiley-VCH, Berlin, 2000).
[33] W. H. Miller, Faraday Discuss. **110**, 1 (1998).
[34] H. B. Wang, M. Thoss, K. L. Sorge, R. Gelabert, X. Gimenez, and W. H. Miller, J. Chem. Phys. **114**, 2562 (2001).
[35] M. Ovchinnikov, V. A. Apkarian, and G. A. Voth, J. Chem. Phys. **114**, 7130 (2001).
[36] M. B. Plenio and P. L. Knight, J. Phys. Chem. A **102**, 4414 (1998).
[37] H.-P. Breuer, B. Kappler, and F. Petruccione, J. Phys. Chem. A **102**, 4414 (1998).
[38] O. Linden and V. May, J. Phys. Chem. A **102**, 4414 (1998).
[39] I. Kondov, U. Kleinekathöfer, and M. Schreiber, J. Chem. Phys. **119**, 6635 (2003).
[40] J. Jean, R. Friesner, and G. Fleming, J. Chem. Phys. **96**, 5827 (1992).
[41] D. Egorova, A. Kühl, and W. Domcke, Chem. Phys. **268**, 105 (2001).
[42] T. Joo, Y. Jia, J.-Y. Yu, M. J. Lang, and G. R. Fleming, J. Chem. Phys. **104**, 6089 (1996).
[43] K. Duppen and D. A. Wiersma, J. Opt. Soc. Am. B **3**, 614 (1986).
[44] T. I. C. Jansen, J. G. Snijders, and K. Duppen, J. Chem. Phys. **113**, 307 (2000).
[45] T. I. C. Jansen, J. G. Snijders, and K. Duppen, J. Chem. Phys. **114**, 10910 (2001).
[46] B. Wolfseder, L. Seidner, G. Stock, and W. Domcke, Chem. Phys. **217**, 275 (1997).
[47] H. Wang and M. Thoss, Chem. Phys. Lett. **389**, 43 (2004).
[48] B. Balzer and G. Stock, J. Phys. Chem. A **108**, 6464 (2004).
[49] T. Renger and V. May, J. Phys. Chem. A **102**, 4381 (1998).
[50] O. Kühn and V. Sundström, J. Chem. Phys. **107**, 4154 (1997).
[51] M. F. Gelin, D. Egorova, and W. Domcke, Chem. Phys. **301**, 129 (2004).
[52] A. V. Pisliakov, T. Mančal, and G. R. Fleming, J. Chem. Phys. **124**, 234505 (2006).

directional information from the total polarization.[30] Once this is established, the NP approach allows a convenient treatment of experimental situations that require an extra theoretical effort if handled perturbatively. For example, in the case of overlapping pulses, perturbative methods need to take into account different time orderings inside the pulse overlap region.[42] The NP approach handles overlapping pulses automatically. Moreover, the NP method may enable the treatment of strong field effects and non-Condon effects and the inclusion of an arbitrary form of dissipation even during the pulses if these are correctly described by the system's equations of motion. While the NP approach provides a convenient and flexible tool for the calculation of nonlinear signals, it provides less guidance for the interpretation of signals in terms of elementary processes than do perturbative methods. Accordingly, we will often use a perturbative terminology to describe and explain the underlying dynamical processes. The method offered here, however, has a clear physical interpretation based on the differences of the phase of the electric field experienced by molecules in different positions in the sample and is related to the interpretation of nonlinear spectroscopy in terms of a dynamic grating.[43] Together with molecular dynamics it may become useful, e.g., for finite field calculations such as those in Refs. 44 and 45.

So far, the NP method has been implemented mainly for the calculation of two-pulse pump-probe signals.[30,46–50] Examples include electron transfer model systems,[46,47] *cis-trans* multidimensional photoisomerization models,[30,48] and photosynthetic antenna complexes.[49,50] Recently, the NP approach was developed for the calculation of time- and frequency-gated spontaneous emission spectra.[51] In this article, we extend the nonperturbative approach to the most general (three-pulse) four-wave mixing (FWM) spectroscopic experiments. The theoretical method is illustrated by the calculation of two-dimensional (2D) spectra of a simple and well understood model two-level system. In paper II[52] of this study, we apply the approach to an excitonically coupled dimer system.

The paper is organized as follows. In Sec. II we discuss three-pulse FWM experiments and define the spectroscopic signals. In Sec. III the main idea of the NP approach is introduced and a method to calculate directional contributions is established. The model molecular system we use for the calculation of the spectroscopic signals and the equations of motion are introduced in Sec. IV. Section V presents the results and discussion of our calculations for the model system.

II. TWO-DIMENSIONAL PHOTON ECHO SPECTRA

Formally, the only difference between the perturbative and nonperturbative approaches is in the treatment of the polarization $P(t)$. As a consequence, the definitions of nonlinear spectroscopic signals remain completely equivalent in the two formulations.

The system-field interaction is described in the semiclassical dipole approximation [see Eq. (1)] where the external electric field $\boldsymbol{\mathcal{E}}(t)$ is comprised of three laser pulses $\boldsymbol{\mathcal{E}}(t) = \Sigma_{n=1}^{3} \mathbf{E}_n(t)$. Each pulse is characterized by its frequency ω_n, wave vector $\mathbf{k}_n$, polarization $\mathbf{e}$, and a complex envelope $E_n(t)$

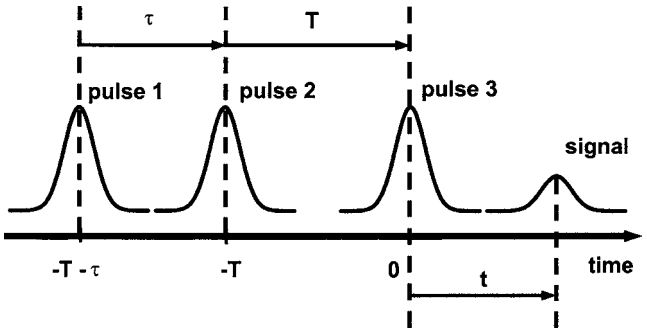

FIG. 1. The pulse scheme of a photon echo experiment. Three pulses with successive interpulse delays τ and T are applied to the system. The time origin is conventionally set to the middle of the third pulse. The photon echo signal arises at times $t>0$. In the 2D spectroscopy we vary the first delay τ to record a two-dimensional signal (in τ and t) for a given delay T.

$$\mathbf{E}_n(t) = \mathbf{l} E_n(t) \exp\{-i\omega_n t + i\mathbf{k}_n \mathbf{r}\} + \text{c.c.} \tag{2}$$

The pulse envelope carries information about the additional time dependent phase modulation and chirp so that it enables us to describe rather complicated pulse forms, provided all envelope changes are slow in comparison with the carrier frequency ω_n.

The photon echo signal detected along the wave-vector direction $\mathbf{k}_s = -\mathbf{k}_1 + \mathbf{k}_2 + \mathbf{k}_3$ results from a system excitation by three pulses centered at times $t = -\tau - T$, $-T$, and 0, with τ and T being the relative delay times described in Fig. 1.

The signal field of the photon echo, $\mathbf{E}_s$, is proportional to the component of the nonlinear polarization in the direction $\mathbf{k}_s$,

$$\mathbf{E}_{k_s}(\tau, T, t) \sim i\mathbf{P}_{k_s}(\tau, T, t), \tag{3}$$

and can be detected using the heterodyne detection scheme described, for example, in Ref. 22. For a given value of the delay, T (population time), between the second and the third pulses in the sequence (see Fig. 1), a 2D spectrum is obtained by successive frequency-resolved measurements of the photon echo signal for different values of the delay τ (coherence time) between the first and the second pulses. Conventionally, one switches to the frequency domain completely by Fourier transforming the spectrum in τ numerically so that the process is equivalent to a double Fourier transform of the time dependent signal

$$S_{2\text{D}}(\omega_\tau, T, \omega_t) \sim \int_{-\infty}^{\infty} dt \exp(-i\omega_t t) \times \int_{-\infty}^{\infty} d\tau \exp(i\omega_\tau \tau) E_{k_s}(\tau, T, t). \tag{4}$$

Here E_{k_s} is related to $\mathbf{E}_{k_s}$ by $\mathbf{E}_{k_s} = \mathbf{m} E_{k_s}$ where $\mathbf{m}$ is a polarization vector of the signal field. The definition of 2D spectra has been discussed in great detail in Refs. 19 and 22. In the frequency domain a 2D spectrum can be easily interpreted intuitively. A 2D spectrum calculated by the procedure described in the next section is a complex valued function, so that one may plot either the absolute value and phase spectra or the real and imaginary spectra. We use the latter representation in this paper.

III. NONPERTURBATIVE CALCULATION OF THE POLARIZATION

The polarization induced by the laser field is defined as an expectation value of the dipole operator

$$\mathbf{P}(t) \equiv \mathrm{Tr}\{\hat{\boldsymbol{\mu}}\rho(t)\}, \tag{5}$$

where the density matrix (DM) $\rho(t)$ is obtained by solving a suitable equation of motion.

In general, the overall nonlinear polarization consists of a number of contributions,

$$\mathbf{P}_{\mathrm{NL}}(t) = \sum_{l,m,n} \mathbf{P}_{lmn}(t)\exp[i(l\mathbf{k}_1 + m\mathbf{k}_2 + n\mathbf{k}_3)\mathbf{r}] + \mathrm{c.c.}, \tag{6}$$

as a result of the system interaction with different wave-vector components of the field. Individual terms can easily be distinguished both experimentally and in a perturbative calculation via the direction of the emitted radiation, $\mathbf{k}=l\mathbf{k}_1+m\mathbf{k}_2+n\mathbf{k}_3$. The photon echo, for example, corresponds to $l=-1$, $m=1$, and $n=1$. In contrast to the experiment, a nonperturbative calculation of the expectation value of the dipole operator [Eq. (5)], gives an *overall* polarization, which is a sum of all contributions. For the case of two pulses and systems with a single optical transition, Seidner *et al.*[30] have developed a method to extract individual components. Our aim is to extend their approach to three-pulse experiments.

We start by formally defining the phase as $\phi_n=\mathbf{k}_n\mathbf{r}$. The polarization can then be written as

$$\mathbf{P}(t;\phi_1,\phi_2,\phi_3) \equiv \sum \mathbf{P}_{lmn}(t)\exp[i(l\phi_1 + m\phi_2 + n\phi_3)], \tag{7}$$

where the phase factors ϕ_n can be considered as parameters of the individual external fields. Thus the overall polarization depends parametrically on a set $\{\phi_n\}$. Equation (7) can be viewed as a Fourier decomposition. Consequently, after calculating the polarization $\mathbf{P}(t;\phi_1,\phi_2,\phi_3)$ for a set of phases (ϕ_1,ϕ_2,ϕ_3), the individual components $\mathbf{P}_{lmn}$ can be obtained from an inverse Fourier transform[47]

$$\mathbf{P}_{lmn}(t) \sim \int_0^{2\pi} d\phi_1 \int_0^{2\pi} d\phi_2 \int_0^{2\pi} d\phi_3 \times \exp[-i(l\phi_1 + m\phi_2 + n\phi_3)]\mathbf{P}(t;\phi_1,\phi_2,\phi_3). \tag{8}$$

This discrete Fourier transform method is equivalent to the method developed by Seidner *et al.*[30] where the individual components are obtained by constructing and solving the algebraic set of equations. As we will show below, in a given order of the nonlinear signal, the number of components present in the signal is limited (to 12 in the case of the third order) and the inversion of the algebraic set of equations [Eq. (7)] is easily accomplished after the polarization is calculated. Note that we have only half of expression (6) in Eq. (7) so that the polarization $\mathbf{P}(t;\phi_1,\phi_2,\phi_3)$ remains complex.

Let us now calculate the number of components appearing in the $(2N+1)$th order polarization $\mathbf{P}^{(2N+1)}(t)$ for the general case of a three-pulse FWM spectroscopic experiment. We discuss even orders only, since the odd ones vanish for random isotropic media with the inversion symmetry.[26] We assume the rotating wave approximation (RWA), which preserves only resonant optical transitions and also prevents us from addressing experiments such as the four-wave sum frequency mixing. In this case, the most general electronic system that can be studied by a $(2N+1)$th order experiment is a ladder of $N+2$ electronic bands (including the ground state) with a transition dipole moment

$$\hat{\boldsymbol{\mu}} = \sum_{a=0}^{N} \boldsymbol{\mu}_{a,a+1}|a\rangle\langle a+1| + \mathrm{c.c.}, \tag{9}$$

where the state vectors $|a\rangle$ represent different bands. For example, the third order nonlinear spectroscopy can reveal information about a system with a ground state and at maximum two bands separated by energy gaps resonant with the laser field. Using a wave function formalism, we can conveniently write the $(2N+1)$th order component of the nonlinear polarization as

$$\mathbf{P}^{(2N+1)}(t) = \sum_{a} \sum_{j=0}^{N-a} \langle \psi^{2(N+a-j)+a}(t) \times |\boldsymbol{\mu}_{a,a+1}|a\rangle\langle a+1|\psi^{(2j+1)+a}(t)\rangle. \tag{10}$$

For $a=0$ we obtain the expression from Ref. 30 for the two-level system. For $a>0$ we construct the expression analogously by assuming there are $j+1+a$ absorption and j emission events on the ket and $N-j$ absorption and $N-a-j$ emission events on the bra side of the expression. Each of the $2N+1$ interactions with a field introduces one of the six phase factors $e^{\pm i\mathbf{k}_1\mathbf{r}}$, $e^{\pm i\mathbf{k}_2\mathbf{r}}$, and $e^{\pm i\mathbf{k}_3\mathbf{r}}$ resulting (without invoking the RWA) in $6\times(2N+1)$ terms in the polarization with wave vectors $\mathbf{k}_s=l\mathbf{k}_1+m\mathbf{k}_2+n\mathbf{k}_3$ such that $|l|+|m|+|n|=2N+1$. As discussed in Ref. 30, the RWA enables a reduction in the number of polarization components necessary to calculate the nonlinear signal, although a full formulation of the nonperturbative approach is in principle possible. For the remainder of this paper we will invoke the RWA, taking into account nearly resonant excitation processes only. With respect to the RWA, the nonperturbative method developed below carriers essentially the same error as perturbative methods. The accuracy of RWA in the context of nonlinear spectroscopy is discussed in detail, e.g., in Ref. 53.

Conventionally, absorption and emission processes in the ket yield the phase factors $e^{i\mathbf{k}_i\mathbf{r}}$ and $e^{-i\mathbf{k}_i\mathbf{r}}$, respectively, while the corresponding bra interactions give the complex conjugate phase factors. For a given transition $|a\rangle\rightarrow|a+1\rangle$ we can derive the overall phase factor of its contribution to the signal analogously to Ref. 30. First, we denote the number of absorption and emission events of the laser pulse having $\mathbf{k}$ vector $\mathbf{k}_1$ in the ket vector as $a^{(1)}_{\mathrm{ket}}$ and $e^{(1)}_{\mathrm{ket}}$ respectively, and similarly for pulses with wave vectors $\mathbf{k}_2$ and $\mathbf{k}_3$ and the bra vector. Thus, we can write for the number of events

neity remains static. If the energy gap evolves between interactions of the sample with the laser pulses, i.e., if the individual molecules change their position in the spectrum (spectral diffusion), we can expect the shape of the homogeneous contribution to be different, and the associated averaging should result in a more symmetric shape of the 2D spectrum.[2,16,62] In particular, one can measure the degree to which the system remains static or, in other words, the degree to which it remembers its original distribution of inhomogeneity by looking at the evolution of the diagonal elongation and the orientation of the line separating the positive and negative features as a function of population time T. In the next section we demonstrate one possible method of including a dynamical inhomogeneity in the nonperturbative calculation.

VI. DYNAMIC INHOMOGENEITY WITH SPECTRAL DIFFUSION

The NP approach fails to correctly describe the spectral diffusion mainly because approaches based on the reduced equation of motion propagate the density matrix using the averaged transition frequencies of the system, whereas the delayed time-domain photon echo effect appears only when we average over an ensemble of dynamics with different transition frequencies. Perturbative approaches correctly average over ensemble dynamics only after the latter have been evaluated formally in the response functions (see Ref. 26). The transition frequency or, in other words, the energy gap between the ground state and the excited state of each molecule also evolves in time. In perturbative calculations this effect is taken into account by the well-known energy gap correlation function[26,63]

$$C(t) = \langle \omega_{eg}(t)\omega_{eg}(0)\rangle, \tag{30}$$

where the energy gap ω_{eg} is defined as $H_e(Q)-H_g(Q)-\langle H_e(Q)-H_g(Q)\rangle = V_e(Q)-V_g(Q)$, and the time dependence denotes the interaction picture with respect to the Hamiltonian $V_g(Q)$. By partitioning the Hamiltonian (17) into the standard system-bath $H_S+H_B+H_{S-B}$ form, we see that $V_g(Q)$ can be identified with the bath Hamiltonian. Thus, Eq. (30) is the correlation function of the time evolution of the transition energy due to the action of the bath. If this evolution can be correctly incorporated into our inhomogeneity averaging process, we should be able to model the dynamic inhomogeneity.

Let us assume that the distribution of the transition frequencies in the ensemble is Gaussian (16) at all times, but particular molecules can change their frequencies so that they diffuse stochastically through the transition frequency space of the ensemble. A simple implementation of such a process is as follows. First, a random number generator produces the initial Gaussian set of transition frequencies for $\mathcal{N}$ molecules. The $\mathcal{N}$ transition frequencies will be sorted from highest to lowest and numbered from 1 to $\mathcal{N}$. In the first step, i.e., at time $t=t_0$, we associate the nth molecule with the nth transition frequency. At later times $t=t_0+\Delta t$, $t_0+2\Delta t, \ldots, t_0+m\Delta t$, we again generate Gaussian sets of transition frequencies for $\mathcal{N}$ molecules and sort them. By associating the nth molecule with the nth transition frequency again we can obtain a small fluctuation of the correlation function (30), but its value stays approximately constant. To allow for a spectral diffusion, it is crucial that at each of the m time points when we generate transition frequencies, we allow the "neighboring" molecules to exchange positions in the distribution with a certain probability, p_{exch}. Depending on this probability, the correlation function (30) decays approximately exponentially with a certain characteristic rate $1/\tau_{\text{corr}}$. Connecting all generated transition frequencies associated with each molecule, we obtain time dependent transition frequencies $\omega_{eg}^{(n)}(t)$, $n=1,\ldots,\mathcal{N}$ that are used in the equations of motion (21). Two-dimensional spectra resulting from such a calculation are presented in Fig. 5. We assume a set of time dependent transition frequencies $\omega_{eg}^{(n)}(t)$ that generate a correlation function decaying with $\tau_{\text{corr}} \approx 1$ ps. Comparing the spectra at times $T=0$ fs and $T=1$ ps, we clearly observe changes in the shape of both the real and imaginary parts of the spectrum associated with the spectral diffusion. The purpose of the above example is simply to illustrate the effect of the spectral diffusion. The statistical behavior of our molecular ensemble is not strictly correct.[64] In practical calculations, one would calculate the fluctuation pathways of individual molecules by means of a stochastic equation of motion, e.g., the Langevin equation, or molecular dynamics in which case a truly microscopic picture can be established.[44,45]

This demonstration suggests that a proper handling of the dynamic inhomogeneity by means of a stochastic description of the energy gap evolution should be possible. An ideal method for the evaluation of the system dynamics would be one that itself includes $\mathcal{N}$ or more separate trajec-

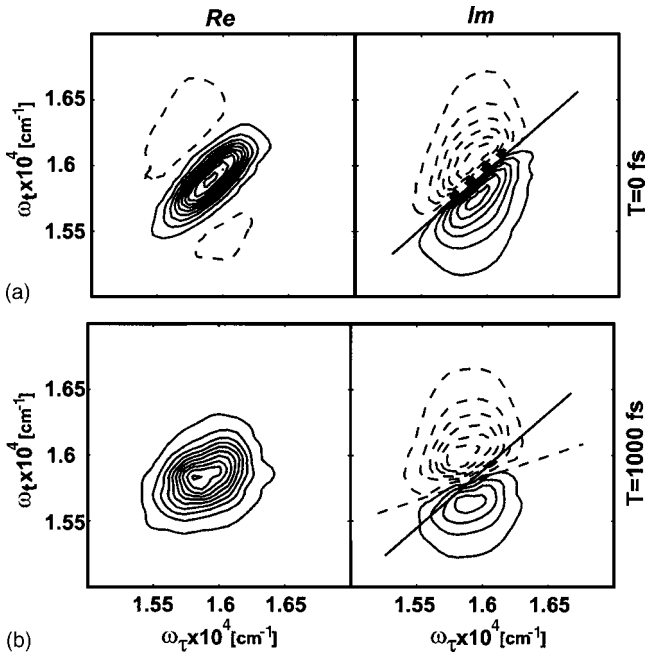

FIG. 5. Two-dimensional spectrum of a two-level system calculated using the stochastic scheme of Sec. VI averaging over 50 molecules. The comparison of the 2D traces at $T=0$ fs and $T=1000$ fs reveals a considerable symmetrization of the real part of the spectrum and a change of the slope of the nodal line in the imaginary part of the spectrum caused by the loss of a system memory. The slope of the nodal line at $T=0$ fs and $T=1000$ fs is represented by continuous and dashed lines, respectively.

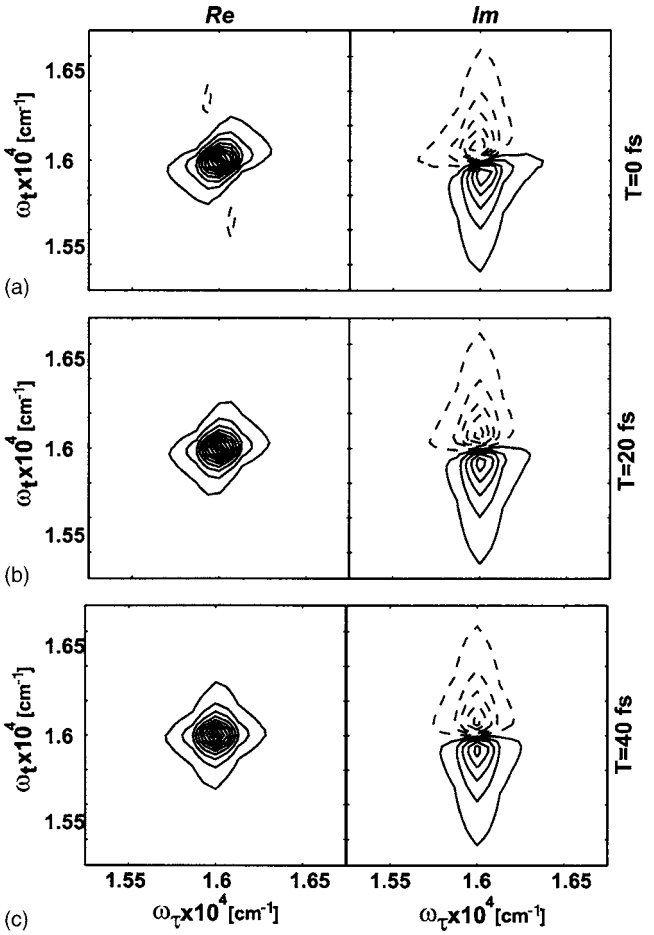

FIG. 3. A sequence of 2D spectra for a homogeneously broadened ($\Delta=0$) two-level system. The population times are $T=0$, 20, and 40 fs; the relaxation parameters are the same as in Fig. 2. Since the duration of the laser pulses is $\tau_{\text{pulse}}=15$ fs, the pulse overlap effects quickly disappear and the traces remain almost unaltered for $T>40$ fs, except for the absolute value of the signal which decreases for increasing T. Contour lines are drawn in 10% intervals at −95% 85%,…, 5%, 5%,…, 95% for the absorptive real parts (left column) and refractive imaginary parts (right column) of $S_{2D}(\omega_\tau, T, \omega_t)$. The 100% level is determined by the highest peak value within the spectrum. Solid contour lines correspond to positive amplitudes, and dashed lines to negative amplitudes.

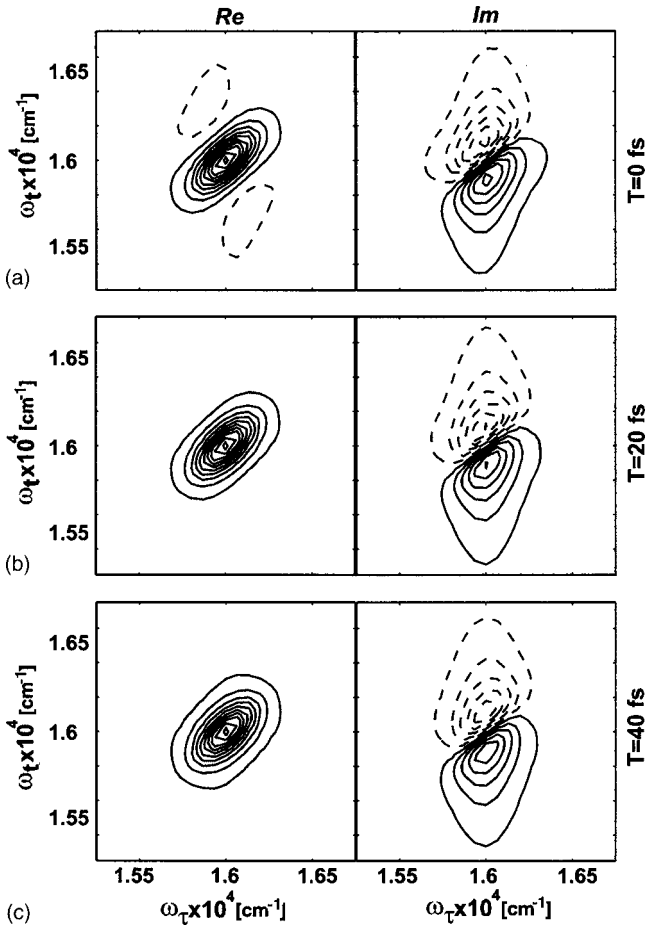

FIG. 4. A sequence of 2D spectra for an inhomogeneously broadened ($\Delta=200$ cm^{-1}) two-level system. All other parameters are the same as in Fig. 3. The inhomogeneous broadening results in a diagonal elongation of the features.

fect by Faeder and Jonas in Ref. 16) and the real parts have weak negative regions for both $\Delta=0$ and $\Delta=200$ cm^{-1}. The effect of the finite laser pulse duration on 2D spectra is clearly visible in both the inhomogeneous and homogeneous examples: as T increases, we can observe the 2D spectra evolving through an intermediate stage at $T=20$ fs [Figs. 3(b) and 4(b)], still in the overlap region, to the "final" shape at $T=40$ fs [Figs. 3(c) and 4(c)], which corresponds to a population time outside the overlap region ($T>\tau_{\text{pulse}}$). We want to stress again that the NP method automatically handles the case of overlapping pulses. For population times larger than the pulse duration [Figs. 3(c) and 4(c)], the real parts of the 2D spectra are entirely positive and the shapes of the 2D spectra are considerably different from the short time shapes. For larger population times the 2D spectra do not change (except the absolute magnitude, which decays due to dephasing).

These final figures represent the intrinsic 2D spectral shapes of both systems. In the case without inhomogeneity [Fig. 3(c)], we observe a highly symmetric shape in both real and imaginary parts. This symmetric "star" shape, a 2D Lorentzian, is characteristic of a homogeneously broadened 2D spectrum.[2,16,62] In the inhomogeneously broadened spectrum [Fig. 4(c)], we see an elliptical diagonal elongation of the real spectrum, together with a diagonal orientation of the nodal line separating the positive and negative features in the imaginary spectrum. The shape of the inhomogeneously broadened spectrum can be easily understood when we realize that the latter can be obtained by adding together many homogeneous spectra, each shifted slightly on the diagonal by its frequency shift value.[2,16,22,62] The homogeneous broadening is responsible for the width of the homogeneous spectral features that is the same in both diagonal and antidiagonal directions. Therefore even the inhomogeneously broadened spectrum reveals the homogeneous contribution in the width of the features along the antidiagonal line.[19] One can understand the orientation of the line separating the positive and negative features in the imaginary part of the spectrum in a similar manner. Such a simple pictorial interpretation of 2D spectral shapes can be applied to more complicated systems as long as we can identify the basic homogeneous spectral shapes. In Paper II of this study we apply this analysis to an excitonic dimer system.

The above discussion is valid as long as the inhomoge-

$$a_{\mathrm{ket}}^{(1)}+a_{\mathrm{ket}}^{(2)}+a_{\mathrm{ket}}^{(3)}=j+1+a,$$

$$e_{\mathrm{ket}}^{(1)}+e_{\mathrm{ket}}^{(2)}+e_{\mathrm{ket}}^{(3)}=j, \tag{11}$$

$$a_{\mathrm{bra}}^{(1)}+a_{\mathrm{bra}}^{(2)}+a_{\mathrm{bra}}^{(3)}=N-a-j+a,$$

$$e_{\mathrm{bra}}^{(1)}+e_{\mathrm{bra}}^{(2)}+e_{\mathrm{bra}}^{(3)}=N-a-j.$$

Using the constraints (11), the overall phase factor of the $(2N+1)$th order nonlinear signal becomes

$$\mathbf{P}^{(2N+1)}(t)\approx e^{i(e_{\mathrm{ket}}^{(1)}-a_{\mathrm{ket}}^{(1)}-e_{\mathrm{bra}}^{(1)}+a_{\mathrm{bra}}^{(1)})(\mathbf{k}_3-\mathbf{k}_1)\mathbf{r}} \times e^{i(e_{\mathrm{bra}}^{(2)}-a_{\mathrm{ket}}^{(2)}-e_{\mathrm{bra}}^{(2)}+a_{\mathrm{bra}}^{(2)})(\mathbf{k}_3-\mathbf{k}_2)\mathbf{r}+i\mathbf{k}_3\mathbf{r}}. \tag{12}$$

All the contributions of j and a have canceled each other in Eq. (12), resulting in the same general formula for the phase factor from all the contributing transitions. Thus, we can write the following expression for the possible $\mathbf{k}$ vectors of the signal field,

$$\mathbf{k}_s=n_1(\mathbf{k}_3-\mathbf{k}_1)+n_2(\mathbf{k}_3-\mathbf{k}_2)+\mathbf{k}_3, \tag{13}$$

where $n_1=e_{\mathrm{ket}}^{(1)}-a_{\mathrm{ket}}^{(1)}-e_{\mathrm{bra}}^{(1)}+a_{\mathrm{bra}}^{(1)}$ and similarly for n_2. We can also formally define $n_3=e_{\mathrm{ket}}^{(3)}-a_{\mathrm{ket}}^{(3)}-e_{\mathrm{bra}}^{(3)}+a_{\mathrm{bra}}^{(3)}$ and note that all three numbers satisfy the relation

$$n_1+n_2+n_3=-1 \tag{14}$$

because for the polarization contribution to be nonzero we require one ket absorption event more than the number of emission events. Since all the a's and e's are non-negative, we can also easily determine the limits for the values of n_a as $\min(n_a)=-N-1$ and $\max(n_a)=N$, $a=1,2,3$. From Eq. (14) we also have $n_1+n_2=-(N+1),\ldots,N$. The conclusion of the above discussion is that the nonlinear polarization of the $(2N+1)$th order (and consequently the emitted electric field of the nonlinear signal) depends only on the relative phases $\delta_1\equiv\phi_3-\phi_1$ and $\delta_2\equiv\phi_3-\phi_2$ of the incoming laser pulses. It is important to note that ϕ_1, ϕ_2, and ϕ_3 are additional phase factors of the pulses resulting from the position $\mathbf{r}$ of the molecular system interacting with the field. All phase factors that the pulses acquire by, e.g., delays in the experimental setup remain unchanged.

For the third-order polarization $\mathbf{P}^{(3)}(t)$ we have $2N+1=3$ and therefore $n_1+n_2=-2$, -1, 0, or 1, giving rise to radiation into 12 directions. We can write down all possible directions: $\mathbf{k}_1$, $\mathbf{k}_2$, $\mathbf{k}_3$, $\mathbf{k}_1-2\mathbf{k}_2$, $\mathbf{k}_1-2\mathbf{k}_3$, $\mathbf{k}_2-2\mathbf{k}_1$, $\mathbf{k}_2-2\mathbf{k}_3$, $\mathbf{k}_3-2\mathbf{k}_1$, $\mathbf{k}_3-2\mathbf{k}_2$, $\mathbf{k}_1+\mathbf{k}_2-\mathbf{k}_3$, $\mathbf{k}_1-\mathbf{k}_2+\mathbf{k}_3$, $-\mathbf{k}_1+\mathbf{k}_2+\mathbf{k}_3$.

The above derivation can be performed with a more complicated form of the dipole operator that provides multiple electronic levels for each band, and the laser field wave vectors $\mathbf{k}_1$, $\mathbf{k}_2$, and $\mathbf{k}_3$ can represent incoming fields of different frequencies. In such a case one needs to track the number of excitations by all three pulses separately, e.g., a_1, a_2, and a_3 instead of a in Eq. (11). In the final expression all contributions of a_1, a_2, and a_3 are canceled, and Eq. (13) remains valid. Caution has to be taken in cases where the frequencies of the incoming fields are multiples of each other, though even here a reformulation of the problem yields Eq. (13) if the $\mathbf{k}_3$ pulse has the lowest frequency. Thus, the nonperturbative method can be applied to the simulation of nondegenerate FWM experiments.

For convenience, we set $\phi_3=0$ and calculate the overall polarization $\mathbf{P}(t;\delta_1,\delta_2)$ for the phases $\delta_{1,2}=m_{1,2}\pi/2$ ($m_{1,2}=0,1,2,3$). Because $\mathbf{P}(t;\delta_1,\delta_2)$ also contains contributions from the lower order of expansion $N=0$ (linear polarization), we need to calculate three linear polarizations (one for each pulse) and subtract these polarizations from the overall polarization

$$\mathbf{P}^{(3)}=\mathbf{P}-\mathbf{P}_{1\ \mathrm{only}}^{(1)}-\mathbf{P}_{2\ \mathrm{only}}^{(1)}-\mathbf{P}_{3\ \mathrm{only}}^{(1)}. \tag{15}$$

The direction-resolved contributions are then obtained from the total nonlinear polarization via the inverse Fourier transform (8).

Although Eq. (6) does not require the applied external electric field to be weak, the subsequent analysis of the directions in which signals of different order travel shows that a weak field has to be applied to prevent higher order signals, significantly influencing the calculation. For example, the photon echo direction in the third order, $-\mathbf{k}_1+\mathbf{k}_2+\mathbf{k}_3$, is the same as the fifth order direction $-\mathbf{k}_1+\mathbf{k}_1-\mathbf{k}_1+\mathbf{k}_2+\mathbf{k}_3$. The problem is, in this respect, similar to the true experimental situation. Since in a computer simulation we have access to information about the population of excited states, we can easily assure the correct weak field conditions.

IV. MODEL SYSTEM AND EQUATIONS OF MOTION

In this section we introduce a simple model system that will provide a basis for development and testing of the method. As the analysis in the previous section shows, the method can be applied to an arbitrary model system, and it does not rely on any particular method of propagation of its equations of motion to calculate the complex polarization of the system induced by the external fields (although in its present formulation it does require the RWA). Here we demonstrate the implementation of the method on a very simple system, an ensemble of molecular systems with only two electronic levels embedded in a solvent. Relaxation (transition from the excited state to the ground state) and dephasing in the system are described by phenomenological rates (see below). Furthermore, we assume that the members of the ensemble experience a range of different environments, resulting in a slight shift of their transition energies. We choose a Gaussian distribution for the transition energies:

$$\sigma(E-E_0)=\frac{\sqrt{\ln 2}}{\sqrt{\pi}\Delta/2}e^{-[(E-E_0)^2/(\Delta/2)^2]\ln 2}, \tag{16}$$

with a full width at half maximum (FWHM) of Δ. The presence of inhomogeneity in the system is vital for the time domain photon echo effect to appear.[26] While pump-probe signals are much less dependent on inhomogeneity, the presence of two time periods that involve the propagation of coherence in the photon echo scheme results in effects that cannot be included directly into the standard equations of motion, as will be shown in Sec. V. Consequently, we have to include inhomogeneity by averaging over a set of individual members of an inhomogeneous ensemble.

The Hamiltonian of a two-electronic-level system can be written simply as

$$H_S = H_g(Q)|g\rangle\langle g| + H_e(Q)|e\rangle\langle e|, \tag{17}$$

with

$$H_1(Q) = \epsilon_i + V_i(Q), \quad i = e,g, \tag{18}$$

where $\epsilon_g(=0)$ is the ground state ($|g\rangle$) electronic energy, $V_g(Q)$ is the nuclear potential energy in the electronic ground state, and Q is the set of all intra- and intermolecular nuclear coordinates (and similarly for the electronic excited state $|e\rangle$). The transition dipole moment operator responsible for coupling to the external electrical field reads

$$\hat{\boldsymbol{\mu}} = \boldsymbol{\mu}_{eg}|e\rangle\langle g| + \boldsymbol{\mu}_{ge}|g\rangle\langle e|. \tag{19}$$

This is the simplest model of a molecular system exhibiting a single electronic transition in the spectral region of interest. The nuclear potentials $V_g(Q)$ and $V_e(Q)$ describe all degrees of freedom (DOF) of the molecule and its environment except the electronic DOF. The Hamiltonian (17) can be easily rewritten in the common system-bath interaction form (see Sec. IV in Paper II). If nonadiabatic terms are present in the Hamiltonian (17), it leads to both relaxation (decay of the diagonal DM element ρ_{ee}) and dephasing (decay of the off-diagonal DM element ρ_{ge}). In this paper we treat the dynamics of the two-level system within the Bloch model: we describe the relaxation and dephasing phenomena by the corresponding population relaxation rate $\gamma = 1/T_1$ and coherence dephasing rate $\Gamma = 1/T_2$, where T_1 and T_2 are the respective decay times. In more elaborate theories these rates can be derived microscopically from a specific form of the system-bath interaction. The total dephasing rate Γ contains a contribution from the population decay of the excited state as well as from the pure dephasing rate $1/T_2^*$ according to[54]

$$\Gamma = \gamma/2 + 1/T_2^*. \tag{20}$$

The equation of motion for the system DM can be written in a general form as

$$\partial_t \rho(t) = -i[(H_S - \boldsymbol{\mu}\cdot\boldsymbol{\mathcal{E}}(t)),\rho(t)] + R\rho(t), \tag{21}$$

where R is the relaxation operator which describes the population decay and coherence dephasing in the system, as specified above. This is a simplified version of the Redfield equation that will be discussed in detail in Paper II. The explicit presence of the system-field interaction term in Eq. (21) underlines the fact that we work within the NP approach.

With the general equation of motion for the DM (21) in hand we can calculate the dynamics of the system under the influence of any type of laser field. From the general form we can derive equations of motion for the elements of the density matrix. Since the method for the extraction of different special components of the polarization has been derived assuming the RWA, we need to introduce this approximation into the equations of motion. Introducing the RWA also provides a numerical advantage as it enables the avoidance of rapidly oscillating terms in Eq. (21) that present a problem for the numerical solution of the equations. The numerical advantage can be quantified by assuming a fixed propagation step method and steps dt_{RWA} for the calculation with the RWA and dt_{full} for the calculation without invoking the RWA. Let us assume that the method needs $N = \tau_p/dt_{\mathrm{RWA}}$ steps within FWHM τ_p of the Gaussian laser pulse envelope. We expect that approximately the same number of steps is necessary to integrate half of the sine wave with a period T_{optical}. If the FWHM of the sine wave is approximated by $T_{\mathrm{optical}}/4$, i.e., $N = T_{\mathrm{optical}}/4dt_{\mathrm{full}}$ the relation between the two time steps is $dt_{\mathrm{RWA}} = (4\tau_p/T_{\mathrm{optical}})dt_{\mathrm{full}}$. Hence, the number of steps needed for a full calculation is $4\tau_p/T_{\mathrm{optical}}$ larger than for the calculation with the RWA.

We assume here that all laser pulses have the same carrier frequency: $\omega_n = \Omega$ for $n = 1,2,3$ (the generalization for the case of different frequencies is rather straightforward). Thus, the electric field can be written as

$$\mathcal{E}(t) = E(t)e^{-i\Omega t} + E^*(t)e^{i\Omega t}, \tag{22}$$

where

$$E(t) = \sum_{n=1}^{3} E_n(t)e^{-i\phi_n}. \tag{23}$$

Invoking RWA means neglecting all terms in the equation of motion that oscillate faster than $e^{\pm i\Omega t}$. Therefore we use the following ansatz for the off-diagonal element of the DM

$$\rho_{eg} = \sigma_{eg}e^{-i\Omega t}. \tag{24}$$

We then obtain the equations of motion where only the slowly varying functions (pulse envelope function $E(t)$ and DM elements σ_{eg}, ρ_{gg}, and ρ_{ee}) are present. We find the following expressions for coherence, excited state population, and ground state population, respectively:

$$\partial_t \sigma_{eg} = -\Gamma\sigma_{eg} + i\mathbf{n}\cdot\boldsymbol{\mu}_{eg}E(t)(\rho_{gg} - \rho_{ee}), \tag{25}$$

$$\partial_t \rho_{ee} = -\gamma\rho_{ee} + i\mathbf{n}\cdot\boldsymbol{\mu}_{eg}E(t)\sigma_{ge} - i\mathbf{n}\cdot\boldsymbol{\mu}_{eg}E^*(t)\sigma_{eg}, \tag{26}$$

$$\partial_t \rho_{gg} = -i\mathbf{n}\cdot\boldsymbol{\mu}_{eg}E(t)\sigma_{ge} + i\mathbf{n}\cdot\boldsymbol{\mu}_{eg}E^*(t)\sigma_{eg}. \tag{27}$$

The closed set of Eqs. (25)–(27) is solved by standard methods with the initial condition (before the first interaction with a field)

$$\rho(0) = \rho_{gg}. \tag{28}$$

The key quantity for calculating nonlinear optical signals of the system is the complex polarization, which for a two-level system is

$$\mathbf{P}(t) = \boldsymbol{\mu}_{eg}\rho_{ge}(t). \tag{29}$$

To utilize the NP method one has to calculate the polarization for a set of different phase relations between the excitation laser pulses. The application of the method can be summarized into the following recipe.

(1) Obtain a system DM by solving equations of motion for a selected set of relative laser pulse phases δ_1 and δ_2.
(2) Calculate $\mathbf{P}(t;\delta_1,\delta_2)$.
(3) Repeat steps 1 and 2 for different values of δ_1 and δ_2; extract the component P_k, according to the method described in Sec. III.

(4) Calculate the desired spectroscopic signal, for example the 2D spectrum (Eq. (4)).

The static inhomogeneity can be simulated by repeating this scheme for different realizations of the Hamiltonian and summing the resulting signals $\mathbf{P}_{k_s}$ before the calculation of the 2D spectrum. Since we have twelve different combinations of δ_1 and δ_2, we need $12\times N$ calculations of the system dynamics to average over N different disorder realizations. However, looking more carefully at the meaning of the phase factors δ_n, we can further optimize the procedure and also obtain physical insight into the NP method. Since the electric field $\mathcal{E}(t)$ is composed of three components [as in Eq. (2)] traveling in directions $\mathbf{k}_1$, $\mathbf{k}_2$, and $\mathbf{k}_3$, the phase relation between the pulses is set to be $\delta_1=\mathbf{k}_3\mathbf{r}-\mathbf{k}_1\mathbf{r}$ and $\delta_2=\mathbf{k}_3\mathbf{r}-\mathbf{k}_2\mathbf{r}$ by the choice of a point $\mathbf{r}$ in the sample. In fact, there is a whole set of equivalent points $\{\mathbf{r}_i(\mathbf{r})\}$ with the same phase relation among the pulses. In other words, choosing 12 different phase relations between pulses and using them to calculate the system dynamics is equivalent to choosing twelve points $\mathbf{r}_1,\ldots,\mathbf{r}_{12}$ in the sample that experience the laser pulses with a given phase relation and calculating the dynamics of 12 ensembles of molecules residing at points equivalent to $\mathbf{r}_1,\ldots,\mathbf{r}_{12}$. Consequently, it is physically more realistic to calculate the polarization for different δ_1 and δ_2 values with a different realization of the Hamiltonian (representing different molecules in the sample) than to repeat the whole calculation scheme given above N times. Thus, in calculations where disorder has to be explicitly taken into account,[55–57] the nonperturbative approach does not represent any computational overhead to the calculation. We will return to this topic later in Sec. VI.

V. 2D SPECTRA OF TWO-LEVEL MODEL SYSTEM: NUMERICAL RESULTS AND DISCUSSION

In this section we illustrate the nonperturbative approach by numerical calculations of 2D photon echo spectra for the two-level model system introduced in the previous section. The two-level system serves as a well-understood reference model for the 2D optical spectroscopy and has been extensively studied within the perturbative approach by Jonas and co-workers[14–19] and recently by our group.[22]

In the two-level model there are only a small number of parameters that influence the shape of the 2D spectra. Most notably, the width Δ of the inhomogeneous distribution of transition frequencies broadens spectral features. An additional contribution comes from homogeneous broadening (dephasing rate $\sim 1/T_2$) which consists of relaxation induced dephasing and pure dephasing [see Eq. (20)]. Because we work in the static inhomogeneous limit, we do not expect the 2D spectrum to present any important dynamic effects for varying population time T, except those arising from the overlap of the laser pulses for times $T<\tau_{\text{pulse}}$ where τ_{pulse} is the width of the pulses used to excite the system. In this simple static model, unlike in the case of the dynamic inhomogeneity,[58] the relaxation of the excited level does not change the shape of the 2D spectrum.

In the calculations that follow, we use a simple fourth order Runge-Kutta (RK) method[59] to solve the equations of motion. The total complex polarization is outputted every 2 fs for τ and t delay times in the interval from 0 to 600 fs. The time step of the RK method is chosen as an integer fraction of the output time and is tested for cumulative error by comparing calculations with different time steps. When the intensity of the absolute value of the laser pulse electric field drops below 0.01% of the maximum of the laser pulse intensity (approximately two times the FWHM from the center of a Gaussian pulse), we invoke a more efficient field-free propagation algorithm based on the diagonalization of the corresponding Liouvian matrix. The photon echo signal is then extracted using the discrete Fourier transform method of Eq. (6). The 2D trace is calculated by a standard fast Fourier transform (FFT) algorithm with a suitable zero padding for times higher then 600 fs. The intensity of the electric field is chosen so that the population of the excited state is less then 1% to ensure that contributions of higher nonlinearities remain negligible.

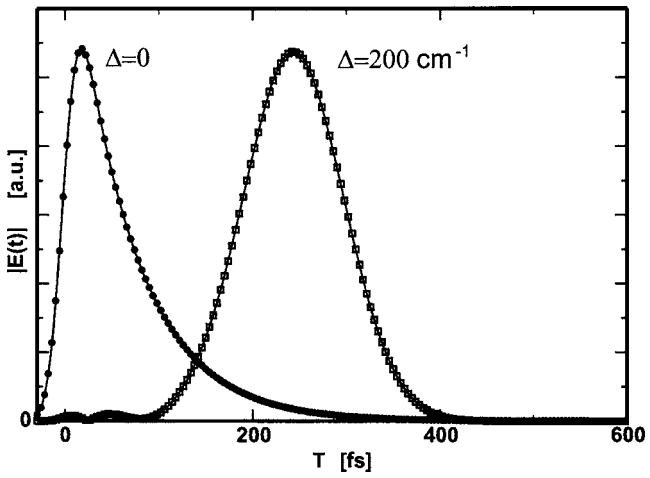

FIG. 2. The time dependent three-pulse photon echo signal of a two-level system calculated for $\tau=300$ fs and $T=1000$ fs. The relaxation and dephasing rates are $\gamma=300$ fs and $\Gamma^*=1/T_2^*=100$ fs, respectively, and the duration of all three laser pulses is $\tau_{\text{pulse}}=15$ fs. Curve (a) presents the homogeneous case with all molecules having a transition frequency $\omega_{eg}=16\,000$ cm^{-1}. Curve (b) shows the signal from an inhomogeneously broadened ensemble with the same mean frequency ω_{eg} and a distribution width (FWHM) $\Delta=200$ cm^{-1}.

Let us first investigate the shape of the three-pulse photon echo signal generated by an ensemble of molecules that all posses the same transition frequency ($\Delta=0$).[26,60,61] The time dependence of the photon echo signal for the coherence time $\tau=300$ fs is presented in Fig. 2. Due to the fact that the ensemble transition frequency has no distribution, there is no rephasing effect, i.e., no delayed photon echo signal appearing around $t=\tau$ (Refs. 26, 60, and 61) as observed in inhomogeneously broadened systems. Figure 2 also presents the time dependent photon echo signal for an ensemble with an inhomogeneous width $\Delta=200$ cm^{-1}. We see that the photon echo signal now appears at $t=\tau$ and later decays due to dephasing.

Calculations for the homogeneous and inhomogeneous systems resulted in the 2D spectra shown in Fig. 3 and 4, respectively. We present a sequence of 2D spectra calculated for various population times T. At $T=0$ [Figs. 3(a) and 4(a)] the spectra are strongly distorted (called a "phase-twist" ef-